# A Neural Network Approach to Radiometric Sensing of Land Surface Parameters

Yuei-An Liou[1], Y. C. Tzeng[2], and K. S. Chen[1]

1. Center for Space and Remote Sensing Research, and
Institute of Space Science
National Central University, Chung-Li, Taiwan (yueian@csrsr.ncu.edu.tw)
2. Department of Electronics Engineering
National Lien-Ho College of Technology and Commerce, Miao-Li, Taiwan

1

## ABSTRACT

**A biophysically-based Land Surface Process/Radiobrightness (LSP/R) model is integrated with a Dynamic Learning Neural Network (DLNN) to retrieve the land surface parameters from its radiometric signatures. Predictions from the LSP/R model are used to train the DLNN and serve as the reference for evaluation of the DLNN retrievals. Both horizontally- and vertically-polarized brightnesses at 1.4, 19, and 37 GHz for an incidence angle of 53 degrees make up the input nodes of the DLNN. The corresponding output nodes compose of land surface parameters, canopy temperature and water content, and soil temperature and moisture (uppermost 5 mm).**

**Under no noise conditions, the maximum of the root mean square (rms) errors between the retrieved parameters of interest and their corresponding reference from the LSP/R model is smaller than 2 % for a four-channel case with 19 and 37 GHz brightnesses as the inputs of the DLNN. The maximum rms error is reduced to within 0.5 % if additional 1.4 GHz brightnesses are used (a six-channel case). This indicates that the DLNN produces negligible errors onto its retrievals. For the realization of the problem, two different levels of noises are added to the input nodes. The noises are assumed to be Gaussian distributed with standard deviations of 1 and 2 K. The maximum rms errors are increased to 9.3 % and 10.3 % for the 1 K and 2 K noise cases, respectively, for the four-channel case. They are reduced to 6.0 % and 9.1 % for the 1 K and 2 K noise cases, respectively, for the six-channel case. This is an implication that 1.4 GHz is a better frequency in probing soil parameters than 19 and 37 GHz. In addition, the promising of the proposed inversion approach on the radiometric sensing of the land surface parameters is demonstrated.**

## I. INTRODUCTION

[1]To appear in *IEEE Trans. Geosce. and Remote Sensing* November 1999.

Land-surface parameters that dominate the partioning of incoming insolation into latent and sensible heat play a crucial role in moisture and energy balance at the lower boundary of atmospheric circulation models [1, 2]. These parameters also govern microwave emission from the terrain. It is hence possible to retrieve the surface parameters from their linkage to the microwave properties [3, 4]. Since the linkage is often extremely nonlinear, it is in general difficult to develop a physically-based retrieval approach.

To resolve the nonlinearity without losing the physical connections, we investigate an indirect approach to infer the parameters by incorporating a physically-based Land Surface Process/Radiobrightnes (LSP/R) model into a Dynamic Learning Neural Network (DLNN). The LSP/R model has been continuously improved over several years. The initial version of the model is developed for a non-freezing, bare soil [5]. It is shortly improved to take into account the freezing of soil moisture [6]. Recently, it has been further improved to accommodate a prairie grassland, and validated by a 7-month fall and winter experiment in grassland near Sioux Falls, South Dakota, during 1992-1993 [7]. The validated LSP/R model provides physical connections between surface parameters and microwave emission of the terrain so that it can be used to verify the retrievals of surface parameters from radiometric characteristics using a neural network approach. Neural networks are known for their capability of handling nonlinear mapping problems. For examples, they are applied to retrieve snow parameters [8], surface wind speeds [9, 10], and relative humidity of the atmosphere [11].

Although numerous studies have demonstrated the strengths of neural networks on the retrieval problems, none of them to our knowledge has been made to link an LSP/R model like ours into a neural network for the retrievals of land surface parameters. In this study, the potential use of the DLNN on retrievals of land surface parameters based on predictions from our LSP/R model is examined.

## II. THE LSP/R MODEL AND THE DLNN

### *A. The LSP/R Model and Its Validation*

The LSP/R model consists of two modules, an LSP module and an R module. The LSP module that treats energy and moisture exchanges between the land and atmosphere, given weather forcings, computes temperature and moisture profiles of the soil and canopy. Energy and moisture transfer in soil and canopy involves solving the 1-dimensional form of the coupled equations [6, 7]

$$\frac{\partial X_{\mathrm{m,\,k}}}{\partial t} = -\nabla \cdot \vec{Q}_{\mathrm{m,\,k}} \tag{1}$$

$$\frac{\partial X_{\mathrm{h,\,k}}}{\partial t} = -\nabla \cdot \vec{Q}_{\mathrm{h,\,k}}, \tag{2}$$

where the subscript k represents the soil or canopy, $X_{\mathrm{m}}$ is the total water mass per unit volume, kg/m$^3$, $X_{\mathrm{h}}$ is the total heat content per unit volume, J/m$^3$, $t$ is the time, s, $\vec{Q}_{\mathrm{m}}$ is the vector moisture (vapor and liquid) flux density, kg/m$^2$-s, and $\vec{Q}_{\mathrm{h}}$ is the vector heat flux density, J/m$^2$-s. The R module manages radiative transfer within canopy, and absorption from the canopy to estimate terrain radiobrightness. The combined soil and canopy radiobrightness is

$$\begin{aligned} Tb = {} & T_{\mathrm{s,\,e}}(1 - R_{\mathrm{p}}(\mu))e^{-\tau_0/\mu} + T_{\mathrm{c,\,e}}(1 - e^{-\tau_0/\mu}) \\ & (1 + R_{\mathrm{p}}(\mu)e^{-\tau_0/\mu}) \end{aligned} \tag{3}$$

| Parameters | AD | SD |
|---|---|---|
| Canopy Temp, K | 1.1 | 1.9 |
| Soil Temp at 2 cm, K | 1.9 | 2.1 |
| Soil Temp at 4 cm, K | 1.8 | 2.0 |
| Soil Temp at 8 cm, K | 1.6 | 1.7 |
| Soil Temp at 16 cm, K | 1.3 | 1.5 |
| Soil Temp at 32 cm, K | 1.1 | 1.2 |
| Soil Temp at 64 cm, K | 0.6 | 0.8 |
| Heat Flux at 2 cm, $W/m^2$ | 4.6 | 6.9 |
| $Tb_s$ at 19.35 GHz, K | -0.06 | 1.1 |
| $Tb_s$ at 37 GHz, K | 6.0 | 2.5 |

Table 1: The AD and SD based upon comparisons between measured and predicted soil temperatures at 2, 4, 8, 16, 32, and 64 cm depths, heat flux at 2 cm depth, and brightnesses at 19.35 and 37 GHz.

where $T_{s,e}$ is the effective emitting temperature of the soil [5, 12], K, $R_p$ is the Fresnel reflectivity of the moist soil for polarization p, $\tau_0$ is the optical thickness of the canopy, $\mu$ is the cosine of $53^0$, the incidence angle of Special Sensor Microwave/Imager (SSM/I), and $T_{c,e}$ is the effective emitting temperature of the canopy, K.

A series of Radiobrightness Energy Balance Experiment (REBEX) were conducted to validate the LSP/R model [13, 14, 15]. REBEX-1 was a 7-month fall and winter experiment in grassland near Sioux Falls, South Dakota, during 1992-1993 [14]. The soil at the REBEX-1 site was a silty clay loam and the grass column density was 3.7 $kg/m^2$. We validated the LSP/R model by forcing the model with observed weather and down-welling radiation during REBEX-1 and comparing model predictions of temperatures, heat flux, and radiobrightness with the corresponding REBEX-1 observations [7]. Observations of a 14-day period from day 287 (October 13, 1992) to day 300 (October 26, 1992) of REBEX-1 are used in the validation. During the period, the grass was green and there was no snow cover. The average of the differences (AD) between model predictions and REBEX-1 observations, and the corresponding standard deviations (SD) are listed in Table 1. In general, the model predictions agree with the corresponding measured values very well. The overestimate of the 37 GHz brightness by 6 K (AD) is caused by scatter darkening that is not considered in the R module.

*B. The DLNN Network*

We treat a nonlinear mapping relation between the radiobrightnesses and the surface parameters by using a Dynamic Learning Neural Network (DLNN) [16]. As in a common practice, the first stage to make the neural network fully and properly operational is to well train it by learning from the data sets that appropriately represent the problem domain. For the feature vector $y \in X$, and output vector $x \in Y$, the goal of the neural network learning is to predict $y$ from $x$ without a priori joint probability distribution. It is achieved by constructing $f : x \longrightarrow y$ such that $f(x)$ well approximates

y, given samples $(x_1, y_1), \cdots,$ and$(x_N, y_N)$, requiring

$$\text{Min}\left[\sum_{i=1}^{N}(y_i - f(x_i))^2\right]. \tag{4}$$

In neural network, no explicit form (non-parameterized type) of $f$ is necessary. Under the framework of DLNN, the learning procedure is illustrated below for reference.

The DLNN indeed is a modified multilayer perceptron in its structure and Kalman filtering technique is used in its learning process [17, 18]. The input-output relationship of the network can be generally expressed as [16]

$$\underline{y} = \underline{W}\underline{x}, \tag{5}$$

where the output vector $\underline{y}$ contains all the output nodes, $\underline{x}$ is a long vector containing all the input and hidden nodes, and matrix $\underline{W}$ is formed by concatenating all the weights that connected to output nodes. This linearization results a modified perceptron structure and thus allows the use of Kalman filtering algorithm to update the weights during learning process. The learning process is terminated according to the following criterion

$$e = \sum_{j=1}^{N}\sum_{k=1}^{c}\frac{1}{2}\|d_k^j - w_k^{N+1}\underline{x}^j\| < \epsilon \tag{6}$$

where $N$ is number of data patterns, $c$ is the total number of the inputs, $d_k^j$ is the $k^{th}$ desired output of the pattern $j$, and $\epsilon$ is a small number. In the crisp network, $d_k^j \in \{0, 1\}$.

The DLNN has the features of fast learning, global minimization, convergence warranty, and built-in optimization of a weighting function at little expense of the computer storage. The fast learning feature stems from the fact that the updating of the weights is accomplished in a global manner avoiding back-propagation, which usually makes the learning process very lengthy.

## III. RETRIEVALS OF LAND SURFACE PARAMETERS

The LSP/R model and the DLNN are integrated to retrieve land surface parameters from terrain brightness temperatures. The land surface parameters of interest are canopy temperature and water content, and soil temperature and moisture (uppermost 5mm). To examine the dependence of the four land surface parameters on frequency, both the four-channel and six-channel cases are studied. According to the Special Sensor Microwave/Imager's configuration [19], both horizontally- and vertically-polarized brightness temperatures at 19 and 37 GHz are utilized for the four-channel case. It has been shown that L-band brightness temperatures are sensitive to soil temperature and moisture over a prairie grassland [7] so that 1.4 GHz horizontally- and vertically-polarized brightness temperatures are used as the additional channels in the six-channel case.

Figure 1 shows the DLNN input-output configurations. The input nodes are the brightness temperatures and the output nodes are the four surface parameters. That is, there are four input nodes for the four-channel case, and six input nodes for the six-channel case. Note that in this study the DLNN contains 2 hidden layers with 40 hidden nodes each (not shown).

The retrieval procedures are shown in Figure 2. Three major steps are proceeded. First, by given surface parameters, the LSP/R model is utilized to simulate a 60-day dry down of a prairie grassland with a column density of 3.7 kg/m$^2$ in summer. In this study, the surface parameters range from about 285 to 305 K for the canopy temperature, 288 to 302 K for the soil temperature, 1.3 to

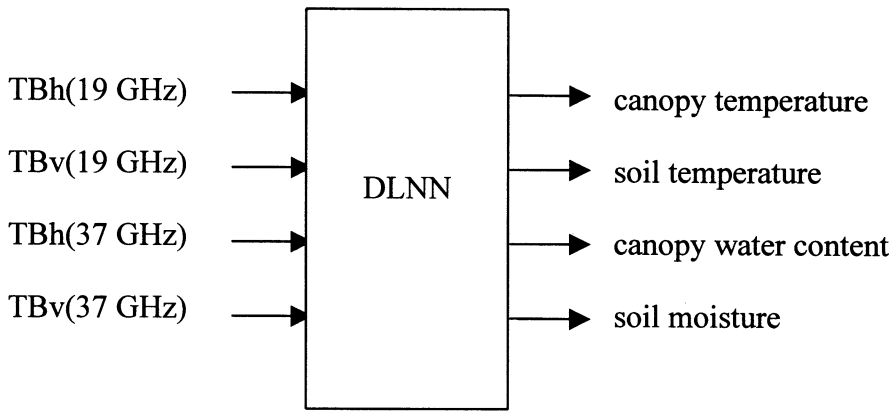


a). four-channel case

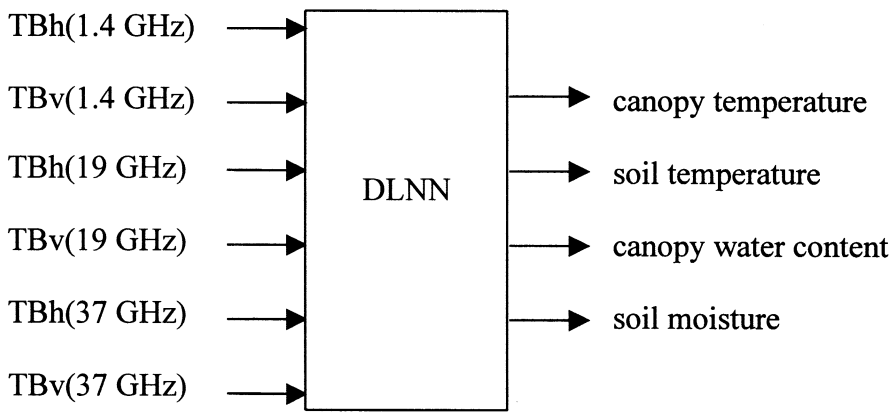


b). six-channel case

Fig.1. The DLNN input-output configurations

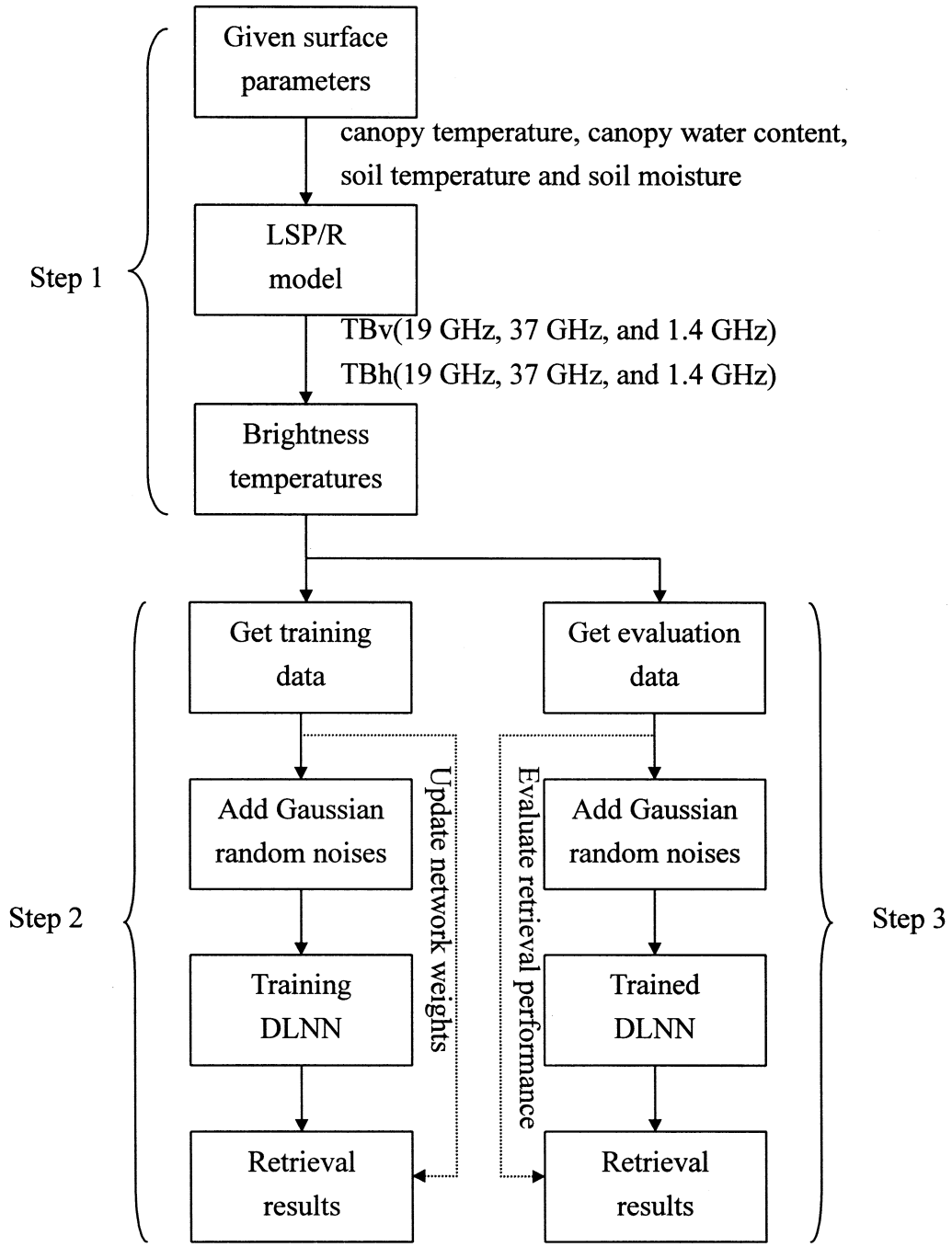


Fig. 2. Retrieval procedures

| Parameters | 4-channel | 6-channel |
|---|---|---|
| Canopy Temp | 100.0 % | 100.0 % |
| Srf Soil Temp | 97.8 % | 99.4 % |
| Canopy Water Content | 99.9 % | 99.9 % |
| Srf Soil Moisture | 97.7 % | 99.9 % |

Table 2: Correlation coefficients between the four- and six-channel DLNN retrievals of canopy temperature, soil temperature, canopy water content, and soil moisture content and their corresponding reference from the LSP/R model for the no noise case.

1.8 kg/m$^2$ for the canopy water content, and 26 to 38 % for the soil moisture. Both horizontally- and vertically-polarized brightness temperatures at 1.4, 19, and 37 GHz for an incidence angle of 53 degree are obtained. A total number of 8640 simulated data was generated. The simulation data are equally distributed in the 60-day period with a temporal spacing of 10 minutes. Second, the LSP/R model predictions are applied to train the DLNN, thus the ground truth can be regarded as fully known. Since the thermal and moisture signatures of the terrain appear periodically, 10 % of the LSP/R model predictions with equal spacings sufficiently represent a complete data set, and, are chosen to train the DLNN.

In addition to the no noise condition, two different levels of random noises are added to the input nodes (brightness temperatures) for the practical consideration. The noises are assumed to be Gaussian distributed with standard deviations of 1 and 2 K. Third, 6 % of the LSP/R model products are randomly chosen to evaluate the performances of the DLNN retrievals.

## IV. COMPARISON BETWEEN FOUR- AND SIX-CHANNEL DLNN RETRIEVALS

The physically-based LSP/R model provides a basis for the inversions. Figure 3 shows the four-channel DLNN retrievals of (a) canopy temperature, (b) soil temperature (uppermost 5 mm), (c) canopy water content, and (d) soil moisture content versus their corresponding reference. In general, the retrieved parameters agree well with the reference. The rms errors between them are small — 0.01 K for the canopy temperature, 0.47 K for the soil temperature, 0.005 kg/m$^2$ for the canopy water content, and 0.05 % (by volume) for the soil moisture content. The corresponding correlations between the retrieved parameters and the reference are high — 97.8 % for the soil temperature, 97.7 % for the soil moisture, 99.9 % for the canopy water content, and 100.0 % for the canopy temperature as given in Table 2.

The six-channel DLNN retrievals of (a) canopy temperature, (b) soil temperature, (c) canopy water content, and (d) soil moisture content versus their corresponding reference for the no noise case are shown in Figure 4. The retrieved parameters agree well with the reference from the LSP/R model. The rms errors between the retrievals and the reference are 0.03 K for the canopy temperature, 0.24 K for the soil temperature, 0.006 kg/m$^2$ for the canopy water content, and 0.1 % for the soil moisture content. The corresponding correlations are also higher — all greater than 99.4 % as given in the Table 2.

A comparison between the four- and six-channel DLNN retrievals reveals two facts. First, the DLNN produces negligible noise on the inversions. Second, the six-channel case gives better inversions than the four-channel case. This illustrates that the 1.4 GHz brightnesses offer more information to

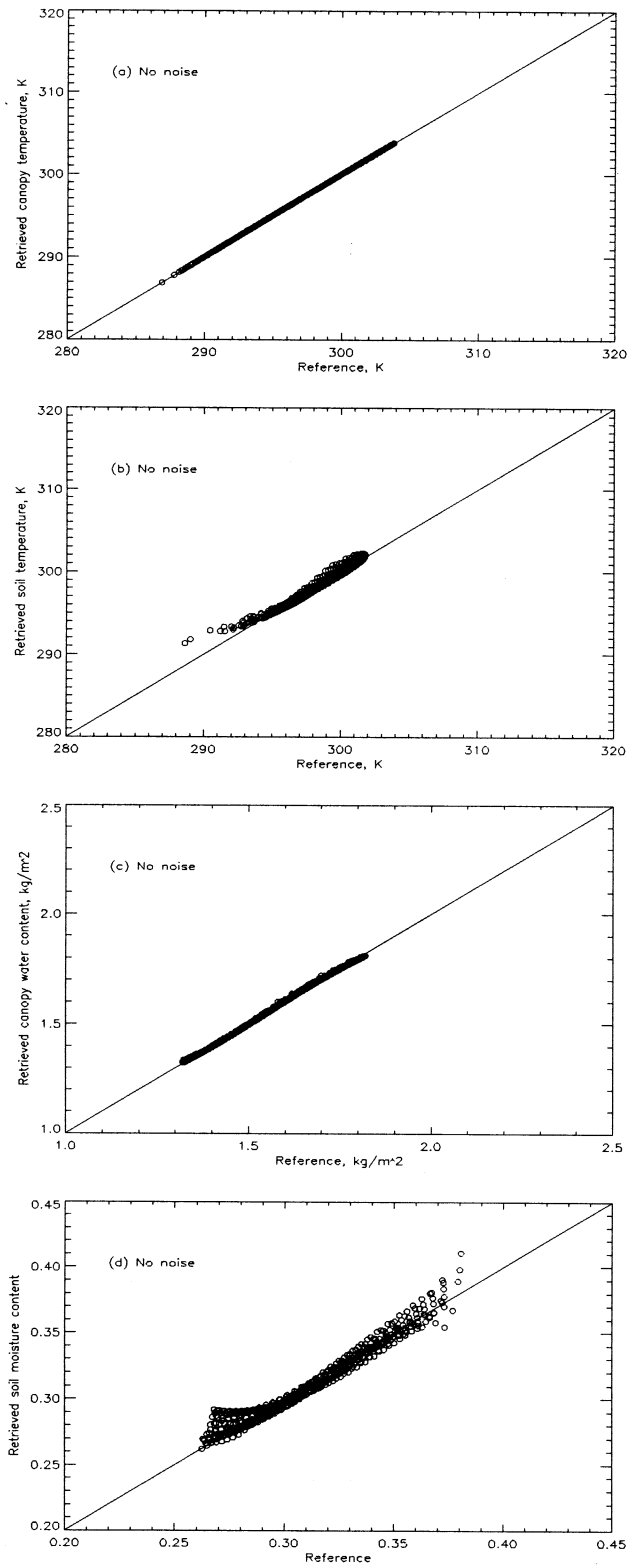


Figure 3: Four-channel DLNN retrievals of (a) canopy temperature, (b) soil temperature, (c) canopy water content, and (d) soil moisture content versus their corresponding reference for the no noise case.

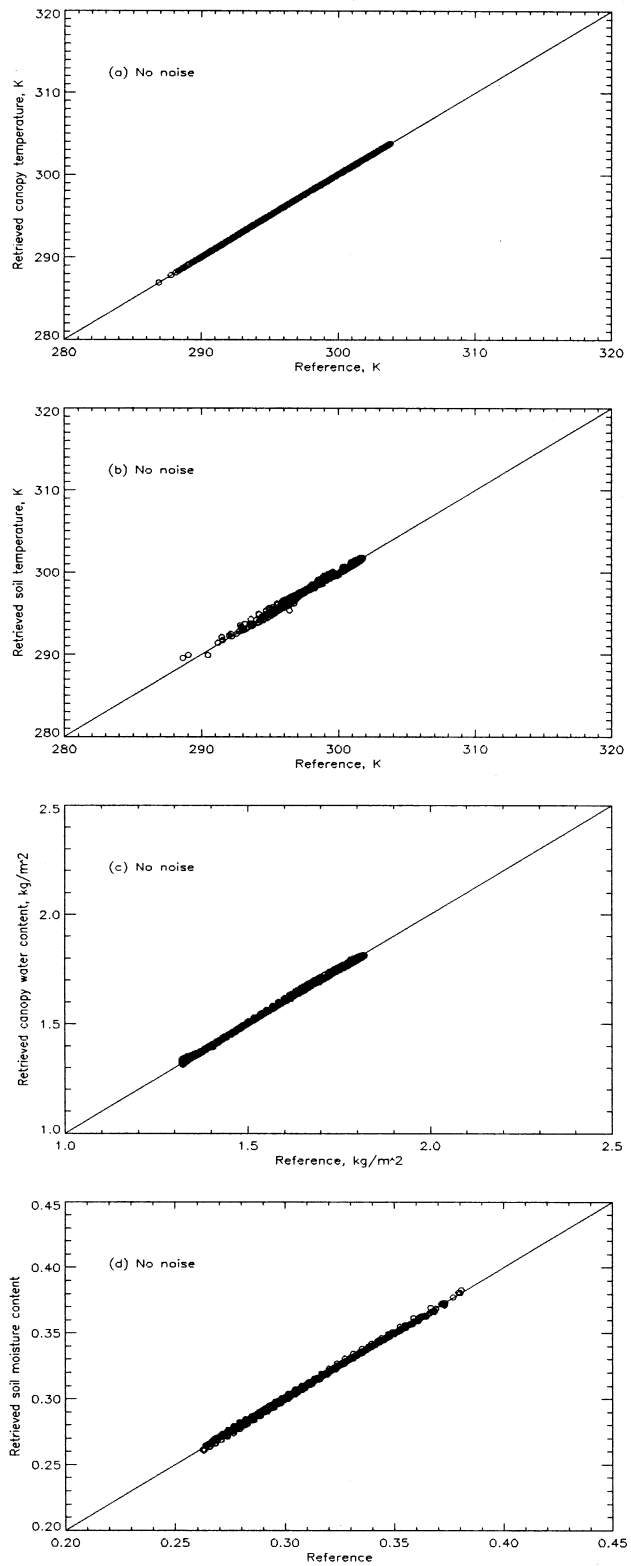


Figure 4: Six-channel DLNN retrievals of (a) canopy temperature, (b) soil temperature, (c) canopy water content, and (d) soil moisture content versus their corresponding reference for the no noise case.

| Parameters | 1 K noise | 2 K noise |
|---|---|---|
| Canopy Temp | 98.7 % | 95.8 % |
| Srf Soil Temp | 77.7 % | 69.3 % |
| Canopy Water Content | 88.6 % | 64.6 % |
| Srf Soil Moisture | 36.6 % | 20.1 % |

Table 3: Correlation coefficients between the four-channel DLNN retrievals of canopy temperature, soil temperature, canopy water content, and soil moisture content with their corresponding reference from the LSP/R model for the 1 and 2 K noise cases.

probe soil properties than the 19 and 37 GHz brightnesses over a grassland with a vegetation column density of 3.7 kg/m$^2$. This is because emissions at 19 and 37 GHz are primarily from the canopy — about more than 90 % for the former and 95 % for the latter, while more than 70 % of terrain emission is from the soil at 1.4 GHz [7]. However, the two "facts" are based on no noise assumptions, which are unlikely to occur in reality. For the realization of the problem, two levels of Gaussian distributed noises with standard deviations of 1 and 2 K are added to the input nodes of the DLNN for both the four- and the six-channel cases.

The four-channel DLNN retrievals of (a) canopy temperature, (b) soil temperature, (c) canopy water content, and (d) soil moisture content versus their corresponding reference for the 1 K noise case are shown in Figure 5. The rms errors between the retrievals and the reference are enhanced to 0.73 K for the canopy temperature, 1.4 K for the soil temperature, 0.08 kg/m$^2$ for the canopy water content, and 2.9 % for the soil moisture content compared to the no noise case. In addition, the corresponding correlations between the retrievals and the reference are degraded, as they should be — 98.7 % for the canopy temperature, 77.7 % for the soil temperature, 88.6 % for the canopy water content, and 36.6 % for the soil moisture content as given in Table 3.

The four-channel DLNN retrievals of (a) canopy temperature, (b) soil temperature, (c) canopy water content, and (d) soil moisture content versus their corresponding reference for the 2 K noise case are given in Figure 6. The quality of the retrievals is further reduced against the no noise and the 1 K noise cases. The rms errors between the retrievals and the reference are 1.3 K for the canopy temperature, 1.6 K for the soil temperature, 0.13 kg/m$^2$ for the canopy water content, and 3.1 % for the soil moisture content. Also, the corresponding correlations become worse as listed in Table 3. The inadequacy of 19 and 37 GHz in sensing soil parameters is gradually becoming obvious for the prairie grassland of this study. Since 1.4 GHz has been recognized as a proper frequency for probing soil state over a grassland, we utilize this frequency in the following analysis.

Figure 7 shows the six-channel DLNN retrievals of (a) canopy temperature, (b) soil temperature, (c) canopy water content, and (d) soil moisture content versus their corresponding reference for the 1 K noise case. As expected, the six-channel DLNN retrievals fit the reference much better than the four-channel DLNN retrievals. We find that the rms errors between the retrievals and the reference are 0.047 K for the canopy temperature, 0.74 K for the soil temperature, 0.072 kg/m$^2$ for the canopy water content, and 0.52 % for the soil moisture content. The corresponding correlations are all higher than 90 % as listed in Table 4.

As the noise level is increased to 2 K, the six-channel DLNN retrievals become less correlated with the reference than the 1 K noise case as given in Table 4. However, they fit the reference much

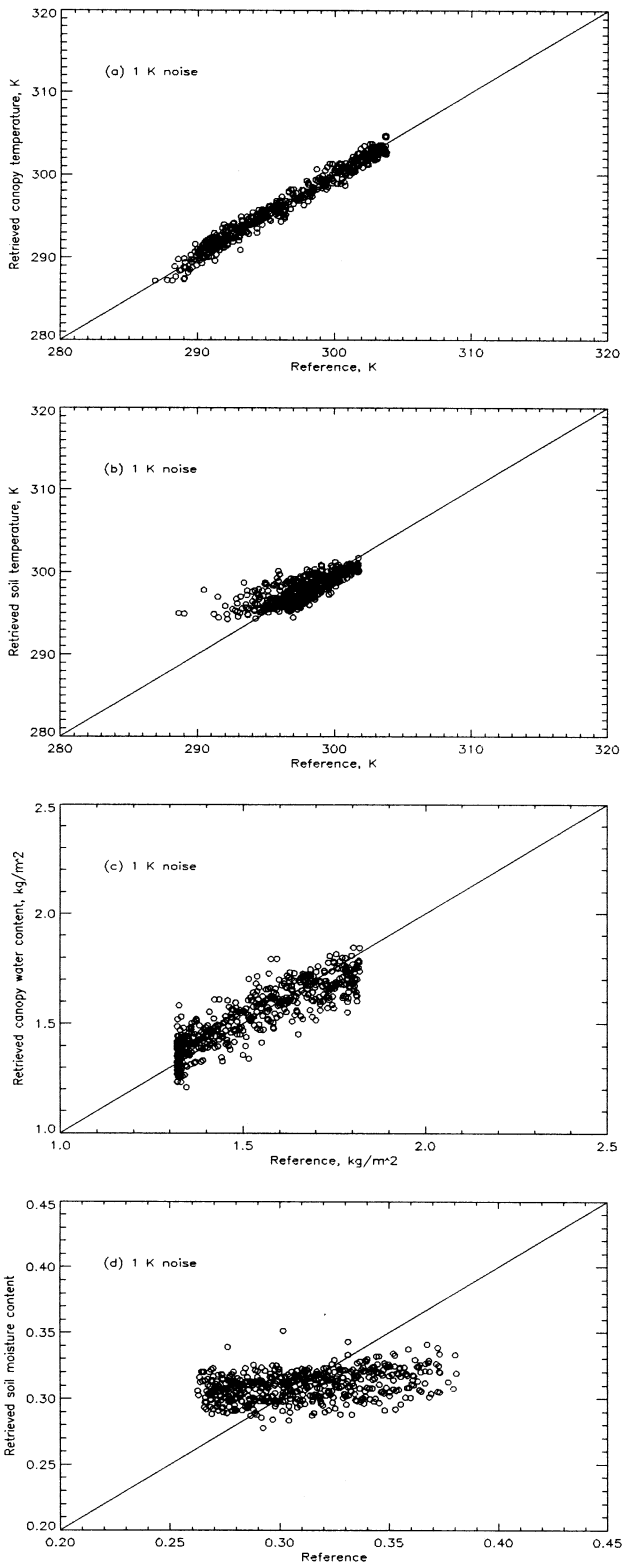


Figure 5: Four-channel DLNN retrievals of (a) canopy temperature, (b) soil temperature, (c) canopy water content, and (d) soil moisture content versus their corresponding reference from the LSP/R model for the 1 K noise case.

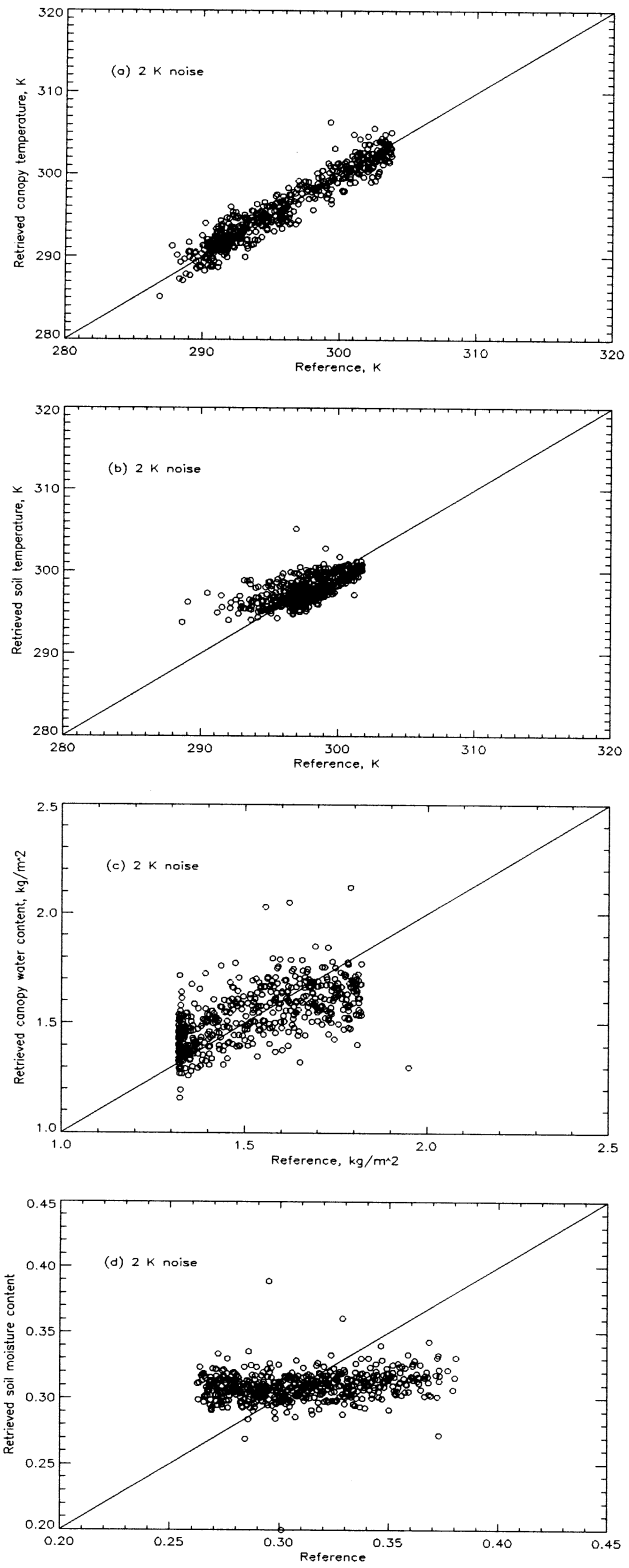


Figure 6: Four-channel DLNN retrievals of (a) canopy temperature, (b) soil temperature, (c) canopy water content, and (d) soil moisture content versus their corresponding reference for the 2 K noise case.

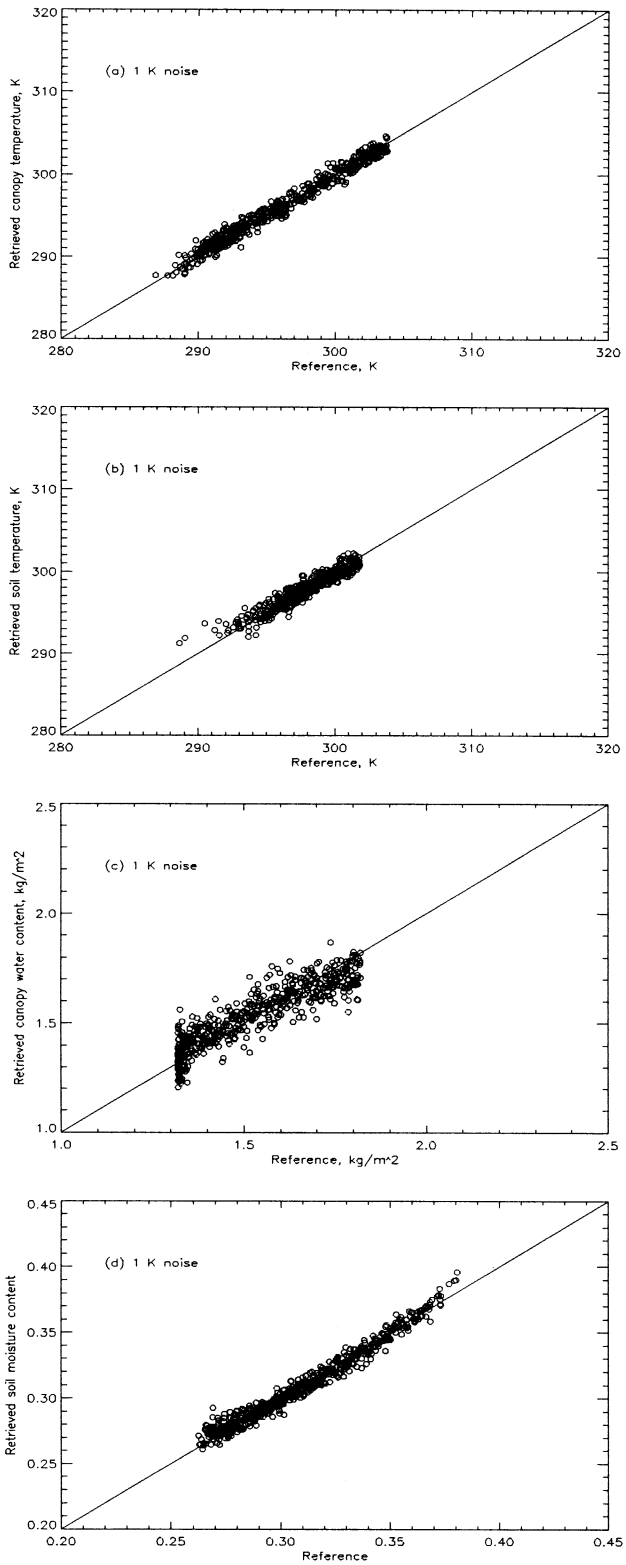


Figure 7: Six-channel DLNN retrievals of (a) canopy temperature, (b) soil temperature, (c) canopy water content, and (d) soil moisture content versus their corresponding reference for the 1 K noise case.

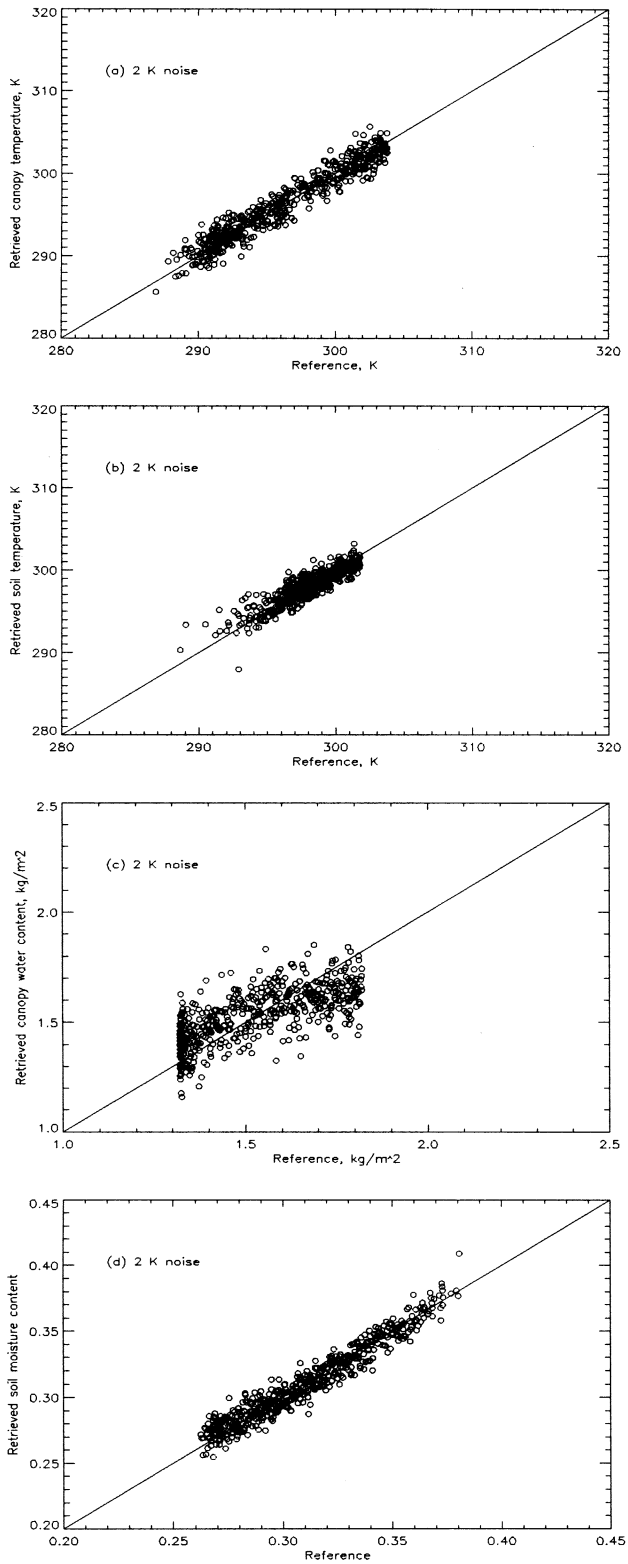


Figure 8: Six-channel DLNN retrievals of (a) canopy temperature, (b) soil temperature, (c) canopy water content, and (d) soil moisture content versus their corresponding reference for the 2 K noise case.

| Parameters | 1 K noise | 2 K noise |
|---|---|---|
| Canopy Temp | 98.9 % | 96.3 % |
| Srf Soil Temp | 94.5 % | 88.6 % |
| Canopy Water Content | 90.3 % | 70.9 % |
| Srf Soil Moisture | 96.7 % | 93.7 % |

Table 4: Correlation coefficients between the six-channel DLNN retrievals of canopy temperature, soil temperature, canopy water content, and soil moisture content with their corresponding reference from the LSP/R model for the 1 and 2 K noise cases.

better than the four-channel DLNN inversions. The corresponding six-channel DLNN retrievals of (a) canopy temperature, (b) soil temperature, (c) canopy water content, and (d) soil moisture content versus their corresponding reference are given in Figure 8.

## V. CONCLUSIONS

A retrieval scheme for the land surface parameters based on a linkage between the LSP/R model and the DLNN is presented. The parameters of interest include the canopy temperature and water content, and the temperature and moisture content of the uppermost 5 mm of soil. The current study has demonstrated that under no noise conditions all of the DLNN retrievals correlate with their corresponding reference from the LSP/R model better than 97.4 % for the four surface parameters for both the four- and six-channel approaches. The four-channel approach utilizes horizontally- and vertically-polarized brightnesses at 19 and 37 GHz, while the six-channel approach includes two additional brightnesses at 1.4 GHz. Clearly, the DLNN introduces negligible noise to the inversions.

For the realization of the practical measurements, Gaussian distributed noises with standard deviations of 1 and 2 K are added to the brightnesses. Although the four-channel DLNN inversions are rapidly degraded, the six-channel DLNN retrievals are reasonably good with correlation coefficients between the retrievals and the reference higher than 80 % for the 2 K noise case. This suggests that the proposed retrieval approach can be powerful in radiometric sensing of the land surface parameters if a proper sensor state is chosen. Integrating the LSP/R model and the DLNN serves as a valuable tool to search such state as well.

## ACKNOWLEDGMENTS

This work has been supported by NSC grants NSC 87-2111-M-008-021 and NSC 88-2111-M-008-031-AP3.

# References

[1] J.-F. Mahfouf, E. Richard, and P. Mascart, "The influence of soil and vegetation on the development of mesoscale circulations," *J. Appl. Meteor.*, **26**, 1483–1495, 1987.

[2] D. P. Rowell, and C. Blondin, "The influence of soil wetness distribution on short-range rainfall forecasting in the West African Sahel," *Q. J. R. Meteorol. Soc.*, **116**, 1471-1485, 1990.

[3] T. J. Jackson, and T. J. Schmugge, "Passive microwave remote sensing system for soil moisture: Some supporting research," *IEEE Trans. Geosci. Rem. Sen.*, **GE-27**, 225–235, 1989.

[4] J.-P. Wigneron, A. Chanzy, J.-C. Calvet, and N. Bruguier, "A simple algorithm to retrieve soil moisture and vegetation biomass using passive microwave measurements over crop fields," *Remote Sens. Environ.*, **51**, 331–341, 1995.

[5] Y.-A. Liou, and A. W. England, "A land surface process/radiobrightness model with coupled heat and moisture transport in soil," *IEEE Trans. Geosci. Remote Sensing*, **36**, 273–286, 1998.

[6] Y.-A. Liou, and A. W. England, "A land surface process/radiobrightness model with coupled heat and moisture transport for freezing soils," *IEEE Trans. Geosci. Remote Sensing*, **36**, 669–677, 1998.

[7] Y.-A. Liou, and A. W. England, "A land surface process/radiobrightness model with coupled heat and moisture transport for prairie grassland," *IEEE Trans. Geosci. Remote Sensing*, 1999. (in press)

[8] L. Tsang, Z. Chen, S. Oh, R. J. Marks II, and A. T. C. Chang, "Inversion of snow parameters from passive microwave remote sensing measurements by a neural network trained with a multiple scattering model," *IEEE Trans. Geosci. Remote Sensing*, **30**, 1015–1024, 1992.

[9] A. P. Stogryn, C. T. Butler, and T. J. Bartolac, "Ocean surface wind retrievals from special sensor microwave imager data with neural networks," *J. Geophys. Res.*, **99**, 981–984, 1994.

[10] K. S. Chen, Y. C. Tzeng, and P. T. Chen, "Retrieval of ocean winds from satellite scatterometer by a neural network," *IEEE Trans. Geosci. Remote Sensing*, 1999. (in press)

[11] C. R. Cabrera-Mercader, and D. H. Staelin, "Passive microwave relative humidity retrievals using feedforward neural networks," *IEEE Trans. Geosci. Remote Sensing*, **33**, 1324–1328, November, 1995.

[12] Y.-A. Liou, and A. W. England, "Annual temperature and radiobrightness signatures for bare soils," *IEEE Trans. Geosci. Remote Sensing*, **34**, 981–990, July, 1996.

[13] E. J. Kim, and A. W. England, "Field data report for Radiobrightness Energy Balance Experiment 0 (REBEX–0), August, 1992 — September, 1993: UM Matthaei Botanical Gardens," UM Radiation Laboratory Technical Report RL-916, August, 1996.

[14] J. F. Galantowicz, (A. W. England, Principal Investigator), "Field data report for the First Radiobrightness Energy Balance Experiment (REBEX–1), October 1992 – April 1993, Sioux Falls, South Dakota," UM Radiation Laboratory Technical Report RL–913, February, 1995.

[15] E. J. Kim (A. W. England, Principal Investigator), "Field data report for the Third Radiobrightness Energy Balance Experiment (REBEX–3), September 1994 – September 1995, wet acidic tundra on the Alaskan North Slope," M Radiation Laboratory Technical Report RL-918, July, 1996.

[16] Y. C. Tzeng, K. S. Chen, W. L. Kao, and A. K. Fung, "A dynamic learning neural network for remote sensing applications," *IEEE Trans. on Geosci. and Remote Sensing*, **32**, 1096-1102, Sept. 1994.

[17] Brown, R. G., and P. Y. C. Huang, *Introduction to Random Signals*, 2nd ed., John Wiley & Sons, Inc., New York, 1992.

[18] S. Haykin, *Neural Networks*, Englewood Cliffs, NJ: Prentice-Hall, 1994.

[19] J. Hollinger, R. Lo, G. Poe, R. Savage, and J. Pierce, *Special Sensor Microwave/Imager User's Guide*, Naval Research Laboratory, Washington, D. C., 1987.